Sandwich panels with stiffeners

André Jorissen[1], Johnny van Rie[2], Thomas Houben[3] and Hèrm Hofmeyer[4]

ABSTRACT: This paper is the third in range presented at WCTE conferences. During the WCTE 2012 in Auckland the paper "sandwich structures with wood-based faces" [1] dealt with the behaviour of traditional sandwich panels. During the WCTE 2014 in Quebec, the paper focussed on these panels with openings for e.g. skylights [2].

In this third paper the modelling of a sandwich panel with stiffeners is analysed. This particular type of sandwich panel promises a considerably higher load bearing capacity, along with other advantages such as less brittle properties, so-called strong points in the structure itself, which allow for connections, and of course the lack of cold bridging as known from other stressed skin and stiffened panels.

The paper presented here can be seen as a report on the research efforts carried out at Eindhoven University of Technology (TU/e), in cooperation with Industry, to provide scientific and experimental background to a building component which is widely used for mainly roof structures. For this, sandwich panels with stiffeners, applied as infill panels and roof panels are analysed analytically, numerically and experimentally.

KEYWORDS: sandwich elements, stiffeners

1 INTRODUCTION

Sandwich panels combine relative high strength and stiffness with high thermal insulation. In the paper called "sandwich structures with wood-based faces" [1], presented at the WCTE 2012 in Auckland, the structural performance of sandwich panels with wood based faces, applied for inclined roofs, was analysed. Additionally, that paper gave special attention to the bi-axial compression stresses at the supports. For the paper called "Sandwich panels with holes" [2], presented at the WCTE 2014 in Quebec City, these traditional elements were further analysed regarding openings for e.g. skylights. To increase strength and stiffness even further, so-called stressed skin panels, see figure 1, can be a solution. However, these panels show areas with reduced thermal insulation, which in turn increases the risk for moisture problems.

[1]André Jorissen, Eindhoven University of Technology (TU/e), Den Dolech 2, 5612 AZ Eindhoven and SHR Timber Research, Nieuwe Kanaal 9b, 6709 PA, Wageningen, The Netherlands. Email: a.j.m.jorissen @tue.nl
[2]Johnny van Rie, Kingspan Unidek, Scheiweg 26, Gemert, The Netherlands. Email:Johnny.vanRie@kingspanunidek.com
[3]Thomas Houben, Eindhoven University of Technology (TU/e), Den Dolech 2, 5612 AZ Eindhoven email:t.w.c.houben@student.tue.nl
[4]Hèrm Hofmeyer, Eindhoven University of Technology (TU/e), Den Dolech 2, 5612 AZ Eindhoven email:h.hofmeyer@tue.nl
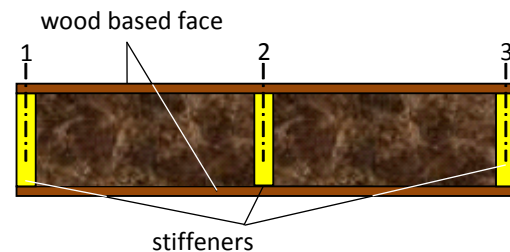
Figure 1: Stressed skin Panel with core stiffeners: 1,2 and 3: areas with reduced thermal insulation

The sandwich panels studied for this paper are similar to the panel shown in figure 2; the reduced thermal insulation in the areas 1,2 and 3 is limited.
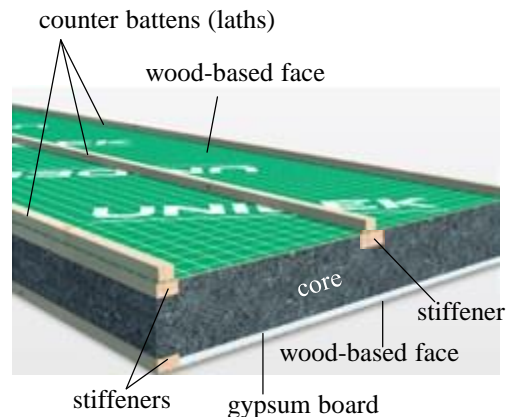

Figure 2: Stiffened Sandwich Panel

The core consists out of rigid foam thermal insulation material, which contain up to 98% of gas (i.e. air, CO_2, Pentane). Consequently, the core shows rather poor structural behaviour. The material does have some compression strength, however the modulus of elasticity and shear modulus are low. Thus, when these panels are loaded in bending, the bending moment is primarily taken by the faces and timber stiffeners.

Shear load is taken by the core (the insulation material) resulting in shear deformation. Whereas for rectangular timber beams shear deformation can normally be neglected (it generally accounts for less than 3% of the total deformation), here shear deformation of the insulation causes more than 30% of the total deflection. Furthermore, due to strengthening of the wood based faces by the added stiffeners, shear failure may be among the expected failure mechanisms. Consequently, shear failure limits the contribution to the strength by the stiffeners.

This paper informs on to what extend the usual approaches for bending stiffness, shear stiffness and effective width are still valid for this particular type of sandwich panel. To verify this, finite element simulations and experimental research has been carried out on four different types of panels, ranging from a normal sandwich (no stiffeners and laths) to a panel with stiffeners, as shown in figure 2 (in which a gypsum board is added for fire resistance).

All analyses described in this paper are based on a so-called four point bending test as shown in figure 3 in which the span $L = 3000$ mm. The load F is applied on the panel, distributed via a hinged bridge structure shown in figure 14 on a distance $a = L/3$ from the end.
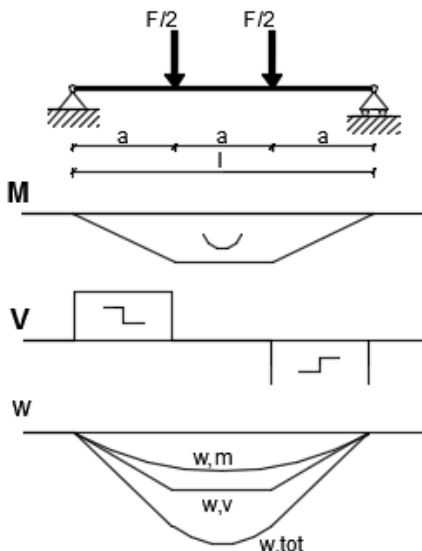

Figure 3: Set-up of the four point bending test

2 THEORETICAL ANALYSES

2.1 Beam theories

Ordinary beam theory (Euler-Bernoulli [3]), shown in figure 4, only takes bending deformations into account by assuming that in the deformed situation cross-sections remain planar and perpendicular to the beam axis. Shear deformations are not regarded.
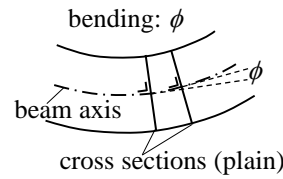

Figure 4: Euler-Bernoulli beam

Here, due to significant shear effects, this ordinary beam theory cannot be applied anymore.
When it is assumed that for shear the relatively stiff wood based faces deform similarly to the core (i.e. cross-section remain planar), as shown in figure 5 on the right, analyses can be carried out according to Timoshenko's [4] theory, shown in figure 6.
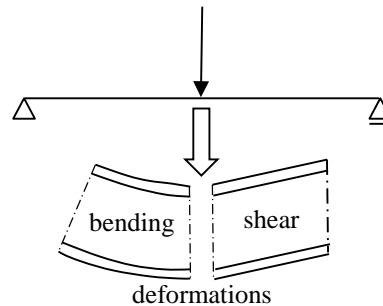

Figure 5: Bending and shear deformations

As mentioned, this is only possible when the wood based faces can be regarded as relatively thin and are able to match the shear deformations. In that case the faces are uniformly loaded in tension or compression (no bending) and the core is uniformly loaded in shear.
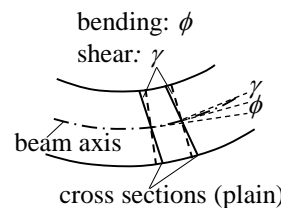

Figure 6: Timoshenko beam; γ is constant over the beam height.

For sandwich elements with rather thick faces it can no longer be assumed that the deformation of the faces is similar to the deformation of the core and a more advanced analysis according to Ready-Bickford, indicated in figure 7, has to be applied [3].
In this case the faces are not loaded uniformly over the face thickness: the faces are loaded in bending as well.
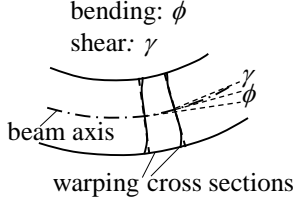
Figure 7: Ready-Bickford beam; γ is NOT constant over the beam height.

It is clear that the selection of either the Timoshenko or the Ready-Bickford model depends on the bending stiffness of the faces; thick faces have a considerable bending stiffness, thin faces have not. Allen [8] defines, that the bending stiffness of the faces (EI_{face}) can be ignored if this is less than 1% of the total panel bending stiffness (EI_{tot}).

The values for EI_{tot} and EI_{face} are explained in figure 8.
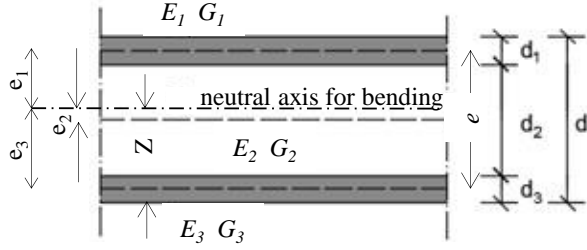
$$EI_{tot} = \sum_1^3 E_i I_i + \sum_1^3 E_i I_i \, e_1^2 \qquad (1)$$

$$E_i I_i = E_i \frac{1}{12} b \, d_i^3 ; \text{faces} : i = 1 \text{ and } i = 3 \qquad (2)$$

$$Z = \frac{\sum_1^3 A_i E_i z_i}{\sum_1^3 A_i E_i} \qquad (3)$$

Figure 8: Bending stiffness of the faces.

The variables in equations (1), (2) and (3) are defined as:

$$e_1 = (d - Z) - \frac{d_1}{2} ; e_2 = Z - d_3 - \frac{d_2}{2} ;$$

$$e_3 = Z - \frac{d_3}{2} ; b = \text{panel width}$$

$$z_1 = d - \frac{d_1}{2} ; z_2 = d_3 + \frac{d_2}{2} ; z_3 = \frac{d_3}{2}$$

$$A_i = \text{panel width} \cdot d_i$$

Remark: the panel width equals $b = 900$ mm or $b = 1020$ mm for the panels analysed.

The four-point bending set-up as shown in figure 3 allows a study of both the bending and shear stiffness separately. For a Timoshenko beam the maximum deflection can be determined using eq. 4.

$$w_{max} = \frac{23}{1296} \frac{F L^3}{EI_{tot}} + \frac{F L}{6 GA_{tot}} \qquad (4)$$

With: w_{max} = maximum deflection (at mid span) [mm]
F = total load applied, see figure 7 [N]
L = span [mm]
EI_{tot} = bending stiffness according to eq. (1)
GA_{tot} = shear stiffness according to eq. (5), based on [5].

$$GA_{tot} = \left(\frac{1}{b e^2} \left(\frac{d_1}{2 G_1} + \frac{d_2}{2 G_2} + \frac{d_3}{2 G_3} \right) \right)^{-1} \qquad (5)$$

Remark: see figure 8 for the symbols used in equation (5).

2.2 Effective width

A so-called effective width is defined for stressed-skin (figure 1) and stiffened panels to model the part of the faces that contribute to the strength and stiffness. In the case of a stressed skin the load carrying part is modelled as an I-shaped cross section of which the flange width equals the effective width described by Möhler [6]. In this study equation (6) from SKH 09-01 [7], resulting in exactly the same values for the effective width as evaluated by Möhler, is used. The effective width according to equation (6) and Möhler are both shown in figure 9.

For the case of the sandwich panels with stiffeners as described in this paper, it is assumed that the effective width approach is valid too, taking into account two aspects. First, it should be checked that the shear stresses in the thin flange (face) do not exceed the shear strength. Second, the flange (face) might suffer from out of plane buckling, however, this is considered not to be relevant here since the flange is fully glued to the core. Consequently, the effective width as defined by equation (6) underestimates the "real" effective width (and is therefore conservative i.c. on the safe side).

$$b_{ef} = \frac{\tanh\left(\frac{\pi}{2} \frac{a_r}{L} \sqrt{\frac{E_{0,panel}}{G_{panel}}} \right)}{\frac{\pi}{2 L} \sqrt{\frac{E_{0,panel}}{G_{panel}}}} \qquad (6)$$

With: b_{ef} = effective width < the spacing between the stiffeners [mm]
a_r = spacing between the stiffeners [mm]
L = span = 3000 [mm]]
$E_{0,panel}$ = Young's Modulus = 2400 [N/mm^2]
G_{panel} = Shear Modulus = 200 [N/mm^2]

$$\frac{b_{ef} \cdot n}{b}$$

L = 3000 mm
b = 1020 mm
n = number of stiffeners

n = 11
n = 6
n = 3   Möhler
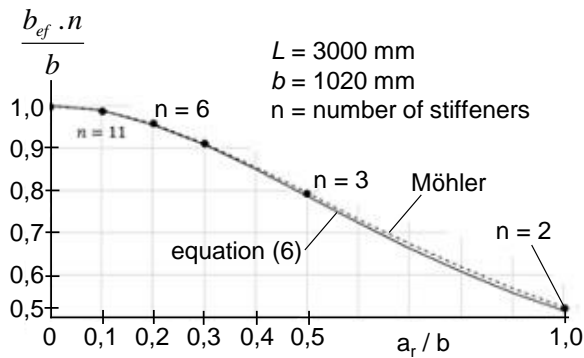equation (6)
n = 2

a_r / b

Figure 9:*Effective width in relation to the distance in between the stiffeners*

3 FINITE ELEMENT SIMULATIONS

In order to study the effects of the stiffeners, a finite element model has been developed (using Abaqus 6.14 standard). The aim was to create a parametric geometrical model, able te model all the variants in this paper. The main aim of the model is to give insight in the local 3 dimensional effects caused by the stiffeners and laths; the question is whether these can be ignored or not. Once the model is validated using experimental results described in this paper, it can be used for different geometries and material properties not included in the experiments.
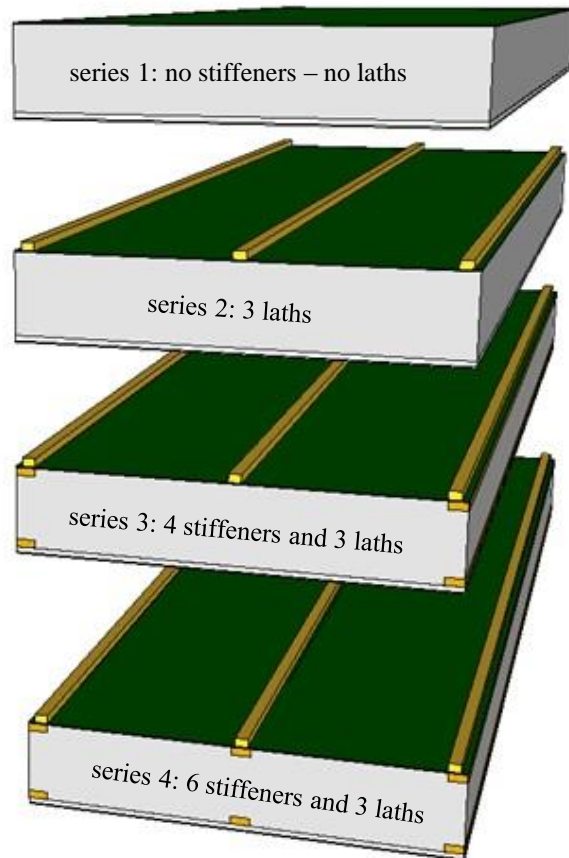
3.1 General

The 3D geometrical models are shown in figure 10; see also figure 2. The span L = 3000 mm.

All simulations are linear elastic. Nonlinear material behaviour is not taken into account and consequently the finite element simulations will deviate from the experimental results as soon as experimental strains surpass the elastic limit.
The Young's modulus and the Shear modulus are used as separate parameters (not depending upon each other); for the face material these values are listed in the legend to equation (4).

3.2 Set up

The model consists of a 3D geometry for which the outer surfaces (faces) are meshed with so-called S4R shell elements. These elements include bending stiffness for the case the face thickness cannot be ignored and use 'reduced integration' and 'hourglass control'. The core of the model is meshed with C3D20R volume elements. These are solid, continuous elements with 20 nodes and 8 integration points. Also here 'reduced-integration' is used.

series 1: no stiffeners – no laths

series 2: 3 laths

series 3: 4 stiffeners and 3 laths

series 4: 6 stiffeners and 3 laths

all elements in a panel are 100% glued together.

Figure 10: *Geometry of the modelled (and tested) panels (see also table 1)*

3.3 Results

As indicated in figure 10, four different types of panels have been simulated. The first panel (series 1) is a normal sandwich with a gypsum board added. The second panel type (series 2) is the same as the first, but now 3 counterbattens (laths) are added. The third panel type (series 3) is the same as the second but now four stiffeners (in the panel courners) are added. The fourth panel type (series 4) is same as the third but with 2 extra stiffeners added (in the middle of the panel).

The geometrical model including the stiffeners and/or laths has not been made conformal. Instead the meshes of the core, faces, stiffeners and laths have been connected by applying so-called "tyings" between the representing geometrical parts. These result in automatically generated couplings and/or constraint equations between the nodes of the different meshes.

Remark: the panels from series 1 are, as expected, by far the weakest and the faces are sensitive to wrinkling due to bi-axial compression in/on the faces at the supports and the load locations as described in [1]. Panels out of series 3 and 4 do not have that particular problem due to the stiffeners and the counterbattens (laths).

Figures 11 (vertical deformations), 12 (longitudinal shear stresses) and 13 (loacal bending stresses) show some results for series 4
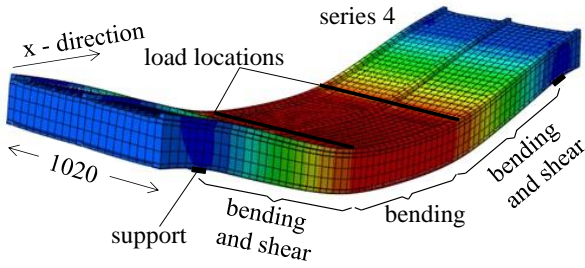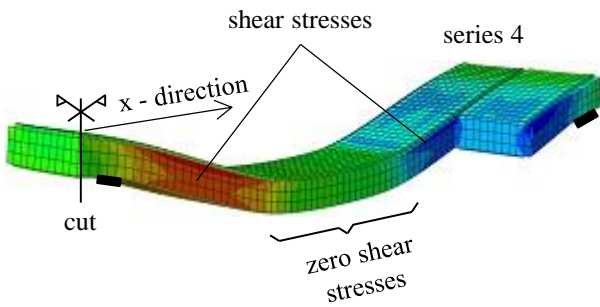

Figure 11: *Vertical displacements.*

Figure 12: *Longitudinal shear stresses.*

In figure 12 both a longitudinal and a cross-sectional cut cut has been made to show that shear stresses differ lengthwise as well as lateral. It seems that at the location of the stiffeners and counter battens (laths), considerable higher shear stresses develop. The shear function is, in principle, the derivative of the bending moment function. Consequently differences in bending stresses along the beam axis (in x-direction) have to be taken care of by shear stresses. Since these differences are high near the stiffeners / counter battens the shear stresses are high at these locations.

In figure 13 the tensile and compression stresses in the cross section at the counter batten and the stiffener of series 4 are presented. The stresses in the faces can be regarded as being constant (due to the low face thickness of 3,2 mm). The stresses in the stiffeners and counter batten are not constant due to the relative high bending stiffness of these elements.

As such Timoshenko's beam theory might not be applicable. This can also be checked using equations (1) and (2) referring to the 1% statement of Allen [8] mentioned in 2.1; the local bending stiffness of the faces (EI_1, equation (2), including the stiffeners and counter battens) reaches about 1,4% of the total panel stiffness EI_{tot} (equation (1)).
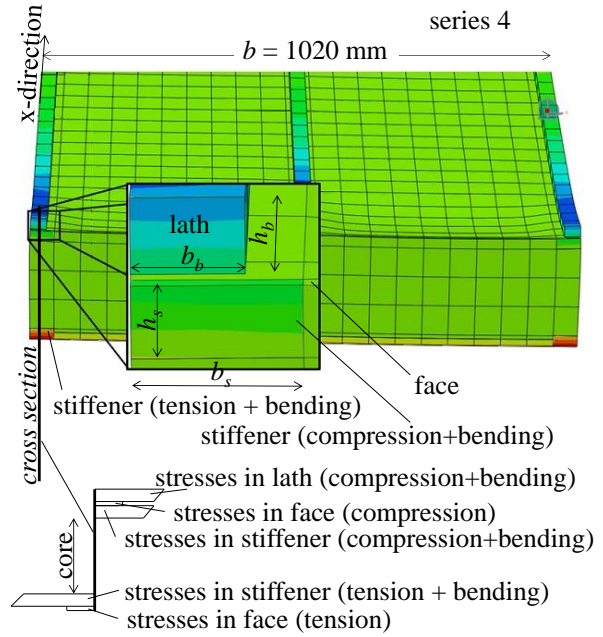

Figure 13: *Bending stressesover the panel thickness at the counter batten location (at x = L/3: near the load introduction)*

4   EXPERIMENTS

Experiments have been carried out in the Pieter van Musschenbroek laboratory of the Eindhoven University of Technology (TU/e). In total 20 specimens have been tested in a four point bending test set up, 5 for each series. Dimensions are presented in table 1, with the span length L = 3000 mm for all series.

Table 1: overview of the samples tested.

series	number of			sample [mm]	
	stiffeners	battens	samples	length	width
1	0	0	5	3500	900
2	0	3	5	3500	900
3	2+2	3	5	3500	1020
4	3+3	3	5	3500	1020

The face material is for all specimen P5 particle board; the core material is EPS 80 (expanded polystyrene with compression strength of 80 kN/m²). The bottom face has a white finish and the top face is green (this causes a slight difference in stress strain relationship; see [9])

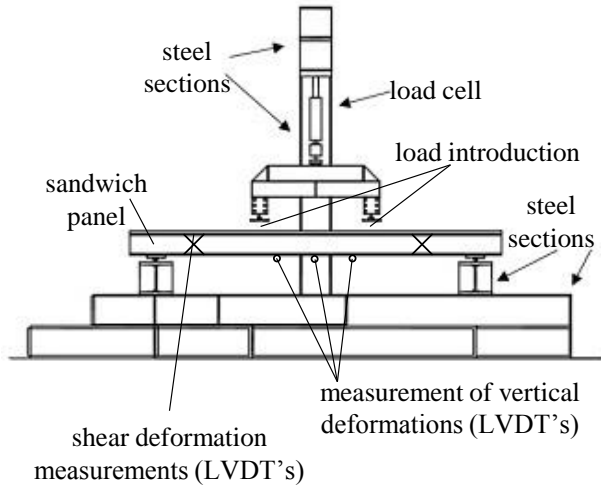The test set up is shown in figure 14.

Figure 14: *Test set up with measurement locations.*

4.1 Shear stiffness measurements

The shear stiffness is measured according EN 408 2010[10] This method uses a diagonal cross along the side of the sample. When the sample is loaded, the diagonals will change in length from which the shear angle and the shear stiffness can be determine; see fig 15 and equations (7) and (8).

$$\gamma = \frac{\alpha \, \Delta V}{GA} = \frac{\Delta w_2 - \Delta w_1}{h_0} \qquad (7)$$

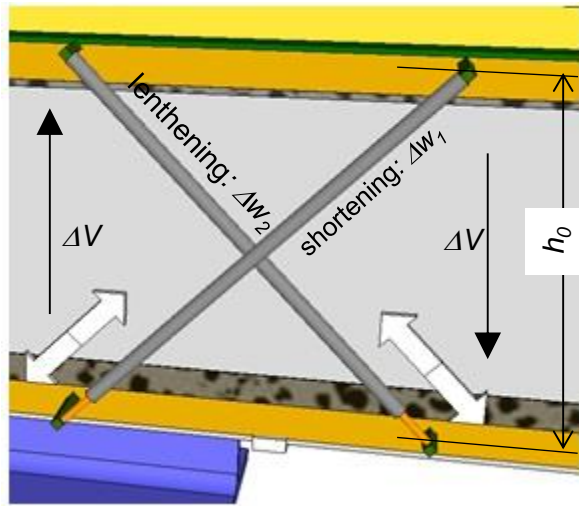$$GA = \frac{\alpha \, \Delta V \, h_0}{\Delta w_2 - \Delta w_1} \qquad (8)$$

Figure 15: *Device for shear stiffness measurement*

With : $\Delta w_{1;2}$ = length change [mm] at of both LVDT's due to a change in shear force

ΔV = change in shear force [N]

α = ratio max shear-to average shear stress

h_0 = projected height between top and bottom of the device

Table 2 shows the results of the shear modulus measurements. In addition, for comparison, the

numerical results and the analytical results according to equation (5) are also shown in table 2.

Table 2: Shear stiffness *GA*

series	shear stiffness GA [kN]		
	experimental equation (8)	numerical FEM	analytical equation (5)
1	457	588	454
2	387	419	454
3	425	468	514
4	436	488	514

It is remarkable that the experimentally and numerically determined shear stiffness for series 2 is lower than for series 1. The reason for this is that the measurement is carried out locally (at the panel edge, where a counter batten (lath) is present). The stresses near the counter batten are higher (as discussed before); the locally higher shear stresses, not accounted for in the global shear load with which *GA* is calculated, result in higher shear deformations and, consequently, a lower *GA* value. In the globally determined *GA* according to equation (5) the total cross section is taken into account and exceeds therefore the experimental and numerical values.

4.2 Deflection

Figure 16 shows the experimental load deformation graphs for all experiments and the average for each series.
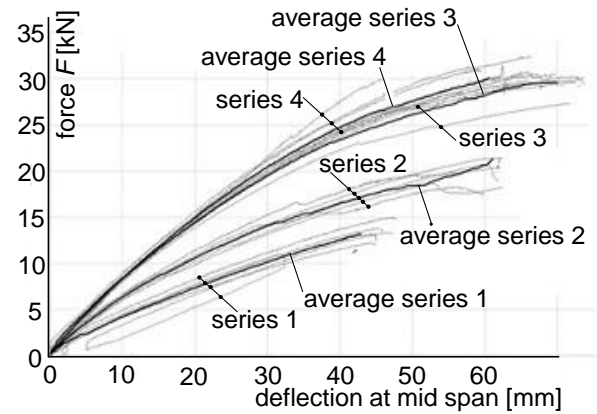

Figure 16: *Load versus displacement: Stiffness*

All the series show a linear-elastic branch, slowly changing in a nonlinear branch, ending with a rather sudden failure.

The failure load is clearly increasing from series 1 to 4. It is remarkable that the difference in between series 3 and 4 is rather small, so the added stiffeners in the middle do not seem to be very effective. Both series 3 and 4 show shear failure in the core material which explains that the load carrying capacity of series 4 is hardly increased compared to series 3.

The experimental results show a slightly more stiff behaviour than is expected according the FEM and the

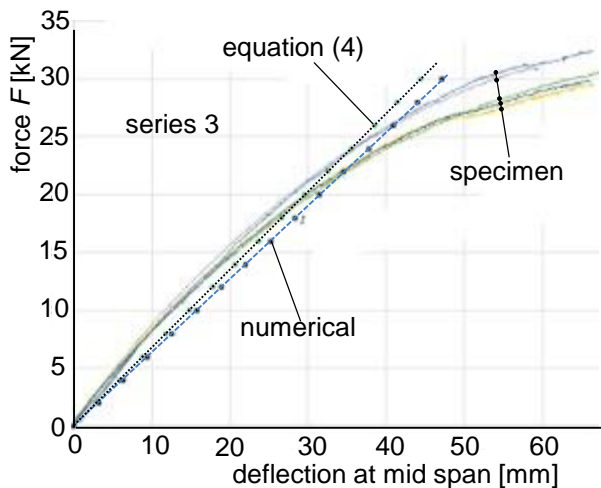analytical values. This is shown in figure 17, as an example for series 3.

Figure 17: *Comparison of the experimental load-slip curves with those determined with FEM analyses and equation (4) for series 3.*

4.3 Strain in the faces

Using strain gauges the strain in the lower face has been measured at mid span. This is particularly interesting for the panels with stiffeners since it is expected that for these the strain varies over the panel width, although, as shown in figure 18, the strain also varies slightly over the panel width for panels out of series 1 (panels without stiffeners).
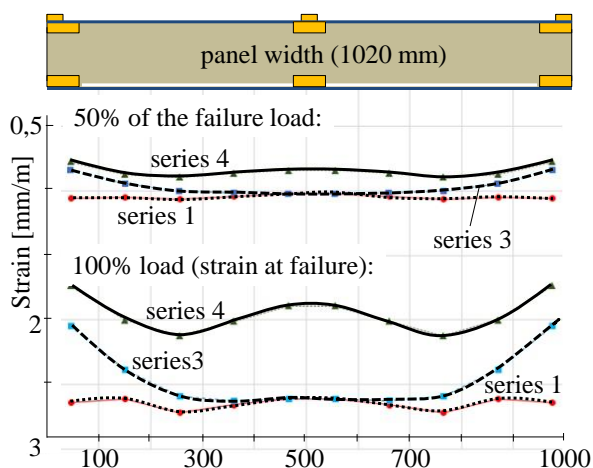

Figure 18: *Strain variation over the panel width at mid span.*

The measuring have been carried out at different lateral distances from the edge of the panel. Figure 18 shows the average strain for series 1, 3 and 4 at 50% and 100% of the maximum load level. Series 1 and 2 have the same configuration at the lower face and show the same result. Series 4 shows the largest variation; due to the fact that this series also has a stiffener in the middle at the bottom face, this is expected (at this location the stiffener restraints the face). Series 3show a maximum strain in the middle (no stiffener present at th bottom face at this location).

In general, it can be seen that the strain is reduced at stiffener locations. This is to be expected since this is actually the background for the effective width described in 2.2.
Figure 16 also indicated that the panel curves (not flat) over the panel width.

5   CONCLUSIONS

The finite element simulations reveal the stresses in the counter battens (laths), faces and stiffeners, among others representing bending stresses, as is shown in figure 13. These local effects are not taken into account in the SKH 09-01 publication [8] (equations (4), (5), (6)). However, the global behaviour of the panel, as expressed in the load-deformation behaviour graphs of figure 15, does not seem to be affected seriously by these local effects.

The shear stresses in the core increase compared to these stresses in panels without stiffeners which may result in shear failure of the core material. Indeed, these failures have been observed during the experiments on panels out of series 3 and 4, which additionally indicate that the extra stiffener applied in the series 4 panels do not or hardly contribute to the load carrying capacity.

Near the stiffeners and counter battens the shear stresses in the faces are much higher compared to the shear stresses in the face materials without the stiffeners. Although a shear or buckling failure due to these higher stresses did not occur during the experiments, this failure mode has to be considered and studied in more detail.

Finally, panels with stiffeners do not remain flat in width direction as indicated by figure 18.

REFERENCES

[1] Jorissen A.J.M., Rie, J.L.G. van, Groot, W.H. de & Luimes, R.A.. Sandwich structures with wood based faces. In Hugh Morris & Pierre Quenneville (Ed.), Oral : Paper presented at *Proceedings of the World Conference on Timber Engineering (WCTE 2012), 15-19 July 2012, Auckland, New Zealand*, (*pp. 202-210*). www.WCTE2012.com, 2012.

[2] André Jorissen, Luc Castelijns, Johnny van Rie and Herm Hofmeyer. Sandwich panels with holes. In Alexander Salenikovich (Ed.), Oral : Paper presented at *Proceedings of the World Conference on Timber Engineering (WCTE 2014), 10-14August 2014, Quebec City, Canada*, 2014.

[3] C. Wang, J. Reddy en K. Lee. Shear deformable beams and plates: relationships with classical solutions. *Elsevier*, Amsterdam, 2000.

[4] Gere J. & S. Timoshenko. Mechanics of materials. PWS Publishing Company, London, 1997.

[5] VandenBossche P. Rapport nr. 3185: Bepalen afschuivingsmodulus met behulp van de vierpuntsbuigproef. *Technisch centrum der houtnijverheid (TCHN)*, Brussels, 2003 (in Dutch).

[6] K. Möhler, G. Abdel-Sayed en J. Ehlbeck. Zur Berechnung doppelschaliger, geleimter Tafelelemente. Calculation of Double-Shell Glued Panels. ISSN: 1436-736X. *Springer*, Karlsruhe, 1963.

[7] A. Jorissen en J. van Rie. SKH-publication 09-01. Praktische rekenmethode voor sandwich en sandwich rib elementen. *SKH*, Wageningen, The Netherlands, 2009 (in Dutch).

[8] Allen H.G. Analysis and design of structural sandwich panels. *Pergamon Press*. London, 1969.

[9] Wim, de Groot. Master thesis. Buigings- en dwarskrachtvervorming van sandwichpanelen. Eindhoven University of Technology. 2008.

[10] EN 408. Timber structures. Structural timber and glued laminated timber. Determination of some physical and mechanical properties. *CEN*, Brussels, 2003.